

RESEARCH PAPER



Synthesis and bioactivities evaluation of oleanolic acid oxime ester derivatives as α -glucosidase and α -amylase inhibitors

Xu-Yang Deng^a, Jun-Jie Ke^a, Ying-Ying Zheng^a, Dong-Li Li^a , Kun Zhang^a, Xi Zheng^b, Jing-Ying Wu^a, Zhuang Xiong^a, Pan-Pan Wu^a and Xue-Tao Xu^a

^aSchool of Biotechnology and Health Sciences, Wuyi University, Jiangmen, P.R. China; ^bDepartment of Chemical Biology, Ernest Mario School of Pharmacy, Rutgers, The State University of New Jersey, Piscataway, NJ, USA

ABSTRACT

Different oleanolic acid (OA) oxime ester derivatives (**3a–3t**) were designed and synthesised to develop inhibitors against α -glucosidase and α -amylase. All the synthesised OA derivatives were evaluated against α -glucosidase and α -amylase *in vitro*. Among them, compound **3a** showed the highest α -glucosidase inhibition with an IC_{50} of 0.35 μ M, which was \sim 1900 times stronger than that of acarbose, meanwhile compound **3f** exhibited the highest α -amylase inhibitory with an IC_{50} of 3.80 μ M that was \sim 26 times higher than that of acarbose. The inhibition kinetic studies showed that the inhibitory mechanism of compounds **3a** and **3f** were reversible and mixed types towards α -glucosidase and α -amylase, respectively. Molecular docking studies analysed the interaction between compound and two enzymes, respectively. Furthermore, cytotoxicity evaluation assay demonstrated a high level of safety profile of compounds **3a** and **3f** against 3T3-L1 and HepG2 cells.

HIGHLIGHTS

1. Oleanolic acid oxime ester derivatives (**3a–3t**) were synthesised and screened against α -glucosidase and α -amylase.
2. Compound **3a** showed the highest α -glucosidase inhibitory with IC_{50} of 0.35 μ M.
3. Compound **3f** presented the highest α -amylase inhibitory with IC_{50} of 3.80 μ M.
4. Kinetic studies and *in silico* studies analysed the binding between compounds and α -glucosidase or α -amylase.

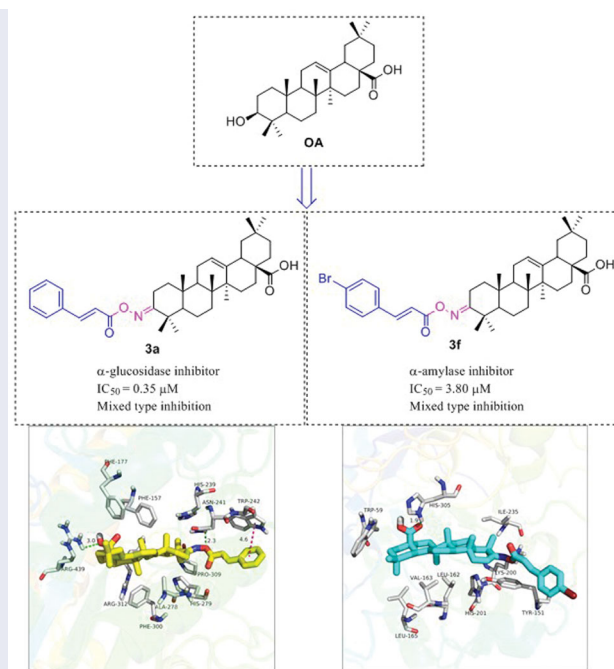
ARTICLE HISTORY

Received 31 August 2021
Revised 7 November 2021
Accepted 10 December 2021


KEYWORDS

Oleanolic acid; structural modification; α -glucosidase; α -amylase; enzyme inhibition

GRAPHICAL ABSTRACT



CONTACT Zhuang Xiong  wyuchemxz@126.com; Pan-Pan Wu  wyuchemwpp@126.com; Xue-Tao Xu  wyuchemxt@126.com  School of Biotechnology and Health Sciences, Wuyi University, Jiangmen, P.R. China

 Supplemental data for this article is available online at [here](https://doi.org/10.1080/14756366.2021.2018682).

© 2022 The Author(s). Published by Informa UK Limited, trading as Taylor & Francis Group.

This is an Open Access article distributed under the terms of the Creative Commons Attribution License (<http://creativecommons.org/licenses/by/4.0/>), which permits unrestricted use, distribution, and reproduction in any medium, provided the original work is properly cited.

1. Introduction

Diabetes mellitus (DM), characterised by chronic hyperglycaemia, has become a serious globalised problem threatening human health¹. It is estimated that more than 460 million people have been suffering from DM with the number of people with DM reaching more than 570 million by 2030². In the light of the causative mechanism, diabetes can be categorised into four classes as follows: type-1 diabetes (T1D), type-2 diabetes (T2D), gestational diabetes (GD) and specific types of diabetes³. As the most common type of diabetes, T2D, resulting from insulin resistance and pancreatic β -cell dysfunction, takes up 90% of all diabetes cases⁴. In addition, the excessive intake in carbohydrates can accelerate the outbreak of T2D⁵. Carbohydrates can decompose into glucose by the synergistic action of several intestinal enzymes, including α -glucosidase and α -amylase, leading to the elevated blood glucose level in the gastrointestinal tract^{6,7}. When carbohydrates are consumed, α -glucosidase hydrolyses carbohydrates to absorbable glucose and α -amylase catalyses the hydrolysis of starch to maltose and glucose⁸. Therefore, the management of T2D can be achieved by reducing postprandial hyperglycaemia through the inhibition of α -glucosidase and α -amylase hydrolysis⁹. Acarbose was the effective clinical hypoglycaemic drugs targeting α -glucosidase and α -amylase. But it still had adverse gastrointestinal side effects, inspiring us to develop new inhibitors.

Oleanolic acid (OA), one of the naturally occurring pentacyclic triterpenoid compounds, was widely found in plant-derived food and medicinal herbs^{10–14}. OA and its derivatives possess different biological activities such as anti-inflammatory, anti-hyperglycaemic, anti-hyperlipidaemic, anti-oxidant and hepatoprotective¹. The research found that the introduction of oxime-ester moiety into OA can improve its anti-tumour activity¹⁵, anti-inflammatory effect¹⁶, the inhibition of HIV-1 protease dimerisation and the inhibitory activity of glycogen phosphorylase compared with the parent compound^{17,18} and other activities, which was presumably associated with the enhancement of the hydrophilic performance¹⁹. Furthermore, our group has been dedicated to the structural modification and derivation of OA skeleton at the C2, C3, C12, C13, or C28 position, simultaneously the inhibition of α -glucosidase and its mechanism have been explored in depth^{20,21}.

Based on the findings above, the conjugation of OA with substituted cinnamic acid and benzoic acid through oxime linkage

have been developed as our ongoing work being aimed to obtain the leading compounds in inhibiting glycosidase. In this study, oleanolic acid oxime ester derivatives **3a–3t** were synthesised by acylation of oleanolic acid oxime, followed by the inhibitory activity evaluation against α -amylase and α -glucosidase.

2. Results and discussion

2.1. Chemistry

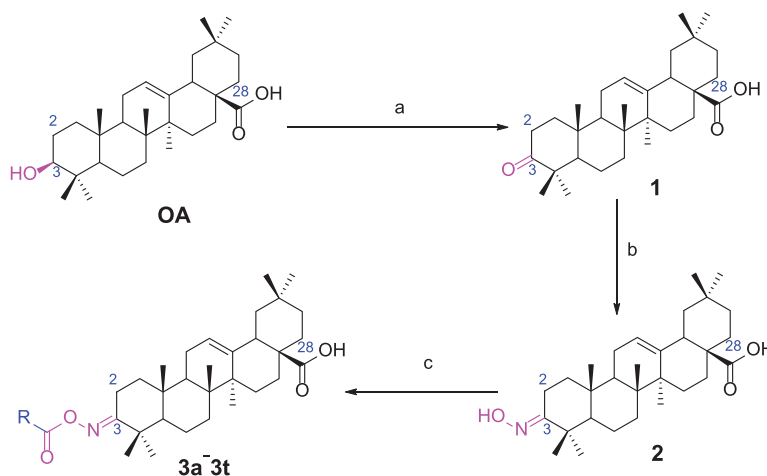
In order to obtain oleanolic acid oxime ester derivatives **3a–3t**, the C3 position of OA scaffold was selected as modification site for the derivation according to the synthetic route concretely depicted in Scheme 1. At first, OA was oxidised to 3-Oxo-olean-12-en-28-oic acid by the freshly prepared Jones reagent, further reacting with hydroxylamine hydrochloride to produce oleanolic acid oxime **2**. Then target compound **3a–3t** were prepared through acylation of the oleanolic acid oxime intermediate **2** with a diversity of cinnamoyl chlorides and benzoyl chlorides. All synthetic derivatives were purified *via* column chromatography and their structures were identified by ¹H NMR, ¹³C NMR and HRMS.

2.2. Inhibitory effect of OA derivatives against α -glucosidase

2.2.1. α -Glucosidase inhibition assay and SAR analysis

The α -glucosidase inhibitory activity of OA derivatives (**3a–3t**) was evaluated with acarbose as the standard inhibitor. As shown in Table 1, all the synthesised OA derivatives (**3a–3t**) had potent inhibitory activity against α -glucosidase with the IC₅₀ values ranging from 0.35 to 3.43 μ M. It was worth noting that all OA derivatives (**3a–3t**) showed stronger inhibitory activity than OA (IC₅₀ = 4.09 μ M) and acarbose (IC₅₀ = 665.56 μ M). Compound **3a** exhibited the strongest inhibitory activity (IC₅₀ = 0.35 μ M), ~11 times stronger than that of OA and ~1900 times stronger than that of acarbose. The results indicated that the introduction of cinnamoyloxyimino moiety at OA-C3 position could enhance the anti- α -glucosidase activity of OA derivatives.

For better understanding the structure activity relationships (SAR), OA derivatives were categorised into two groups, including **A** group (OA derivatives **3a–3j**) and **B** group (OA derivatives **3k–3t**). In **A** group, derivative **3a** was selected as template compound, it could be seen that the introduction of functional groups



Scheme 1. Synthesis of oleanolic acid oxime ester derivatives (**3a–3t**). Reagents and conditions: (a) Jones reagent, acetone, 0 °C; (b) NH₂OH·HCl (1.0 eq.), EtOH, NaOAc (2.0 eq.), rt, 1 h; (c) cinnamoyl chlorides and benzoyl chlorides (2.0 eq.), pyridine, DCM, 0 °C ~ rt, overnight.

Table 1. Inhibition of all the synthesised OA derivatives against α -glucosidase and α -amylase.

Compounds	R	α -Glucosidase inhibition (IC ₅₀ : μ M)	α -Amylase inhibition (IC ₅₀ : μ M)
3a		0.35 \pm 0.06 ^a	7.86 \pm 1.24 ^a
3b		0.68 \pm 0.03 ^a	15.26 \pm 1.41 ^a
3c		0.89 \pm 0.07 ^a	25.37 \pm 1.17 ^a
3d		1.45 \pm 0.12 ^a	17.47 \pm 1.52 ^a
3e		0.95 \pm 0.06 ^a	5.64 \pm 1.29 ^a
3f		1.28 \pm 0.03 ^a	3.80 \pm 0.65 ^a
3g		3.13 \pm 0.13 ^a	12.57 \pm 2.37 ^a
3h		1.36 \pm 0.03 ^a	18.29 \pm 1.92 ^a
3i		0.71 \pm 0.02 ^a	17.87 \pm 1.21 ^a
3j		0.82 \pm 0.09 ^a	70.81 \pm 2.31 ^a
3k		0.67 \pm 0.04 ^a	25.57 \pm 1.66 ^a
3l		0.99 \pm 0.05 ^a	55.30 \pm 2.39 ^a
3m		1.10 \pm 0.10 ^a	35.47 \pm 2.41 ^a
3n		1.96 \pm 0.25 ^a	70.21 \pm 2.53 ^a
3o		1.74 \pm 0.14 ^a	26.32 \pm 1.61 ^a
3p		1.81 \pm 0.05 ^a	15.93 \pm 1.75 ^a
3q		3.43 \pm 0.17 ^a	33.61 \pm 1.93 ^a
3r		1.41 \pm 0.12 ^a	70.72 \pm 1.25 ^a
3s		1.37 \pm 0.06 ^a	18.68 \pm 1.29 ^a

(continued)

Table 1. Continued.

Compounds	R	α -Glucosidase inhibition (IC ₅₀ : μ M)	α -Amylase inhibition (IC ₅₀ : μ M)
3t		0.91 \pm 0.04 ^a	152.36 \pm 4.24 ^a
OA		4.09 \pm 0.11 ^b	94.10 \pm 1.72 ^b
Acarbose		665.56 \pm 13.92 ^c	100.01 \pm 2.73 ^c

Values are the mean \pm SD. Mean values in the same column having different letters are significantly different ($p < 0.05$).

(methyl, methoxy, fluorine, chlorine, bromine, trifluoromethyl, nitro, methylenedioxy and hydroxyl) at C4 position belonging to the cinnamoyl group, weakened inhibitory activity compared with the unsubstituted compounds **3a**. In **B** group, derivative **3k** was selected as template compound, and found the similar results with **A** group that is introduction of functional groups weakened inhibitory activity. Besides, OA derivatives in **A** group had a higher inhibitory activity than OA derivatives with the same substituent in **B** group, respectively. Thence, the incorporation of cinnamoyloxyimino moiety into the OA parent structure could improve the inhibitory activity of OA derivatives better than that of benzoyl groups.

2.2.2. Inhibitory kinetic analysis

To probe into the inhibition mechanism of OA derivatives (**3a–3t**) against α -glucosidase, compound **3a** with the strongest inhibitory activity was selected as the representative compound for the enzyme inhibitory kinetic analysis. The plots of V vs. $[E]$ with or without the presence of compound **3a** (Figure 1(a)) generated straight lines which all passed through the origin, suggesting that the inhibition of compound **3a** was reversible. The inhibition kinetic behaviours were investigated using the Lineweaver–Burk plots. The plots of $1/V$ vs. $1/[S]$ with or without the presence of compound **3a** gave straight lines intersecting in the second quadrant, indicating compound **3a** was mixed-type inhibitor (Figure 1(b)). These results revealed that compound **3a** inhibited α -glucosidase by binding with free enzyme, as well as enzyme–substrate complex.

2.2.3. Docking simulation for α -glucosidase

Docking simulation was performed to clarify the interactions between compound and active pocket of α -glucosidase. The most potent compound **3a** was docked in the active site of α -glucosidase. As shown in Figure 2(a,b), compound **3a** was well nested into the active site, and OA part located inside of the active site. The detailed interaction results between compounds **3a** with active site residues were shown in Figure 2(c,d) using 3D and 2D views, respectively. The carboxylic oxygen at OA part formed a hydrogen bond with Arg439 (3.0 Å), esteryl oxygen at cinnamic acid part made a hydrogen bond with Asn241 (2.3 Å), cinnamic acid benzene ring had a π - π interaction with Trp242 (4.6 Å), and hydrophobic interaction with Phe157, Phe177, His239, Ala278, His279, Phe300, Pro309, and Arg312. The binding affinity of compound **3a** regarding α -glucosidase was -3.7 kcal/mol. Furthermore, the physicochemical properties of most potent compound **3a** was listed in Table 2.

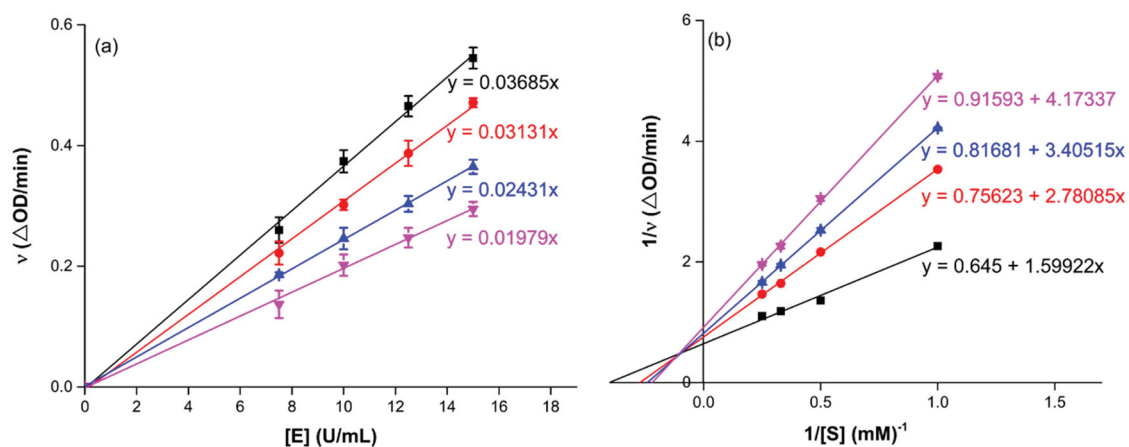


Figure 1. Inhibition kinetics of **3a** on α -glucosidase. (a) The plots of enzymatic reaction rate vs α -glucosidase concentration with or without the presence of **3a**; (b) Lineweaver–Burk plots of enzymatic reaction rate versus substrate concentration with or without the presence of **3a** (**3a** concentration: black line, 0 μ M; red line, 0.25 μ M; blue line, 0.45 μ M; pink line, 0.5 μ M).

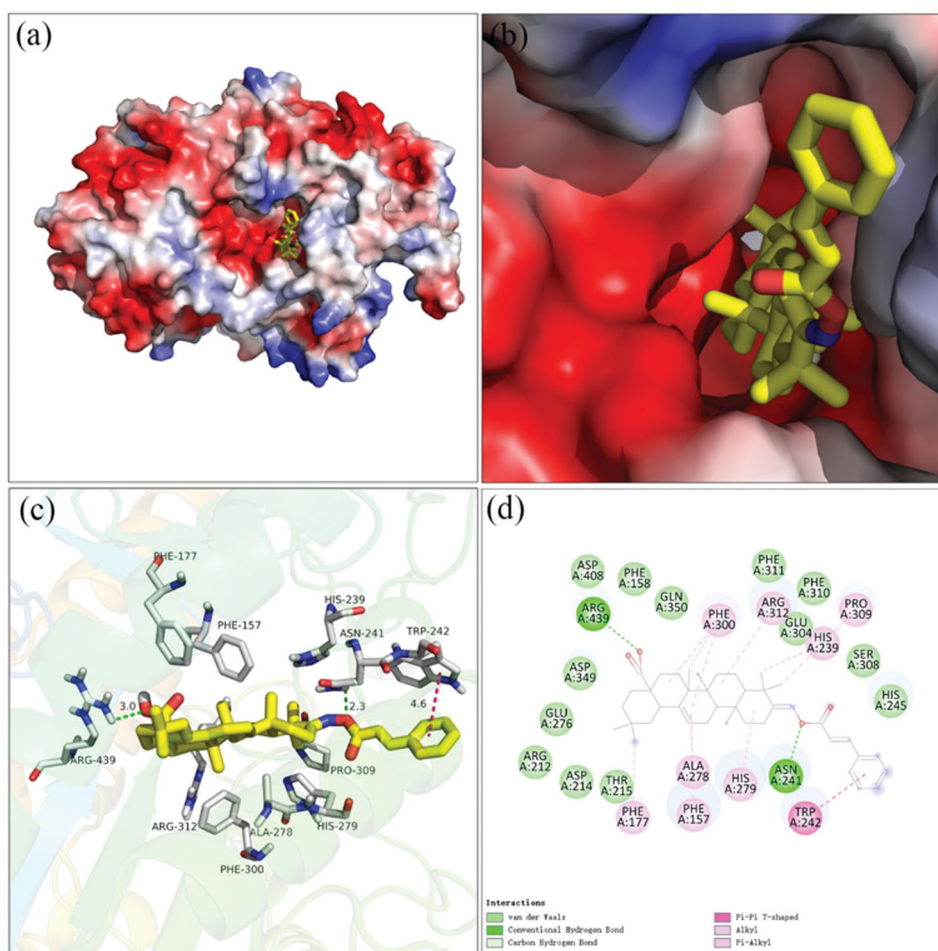


Figure 2. The molecular docking of analogue **3a** with α -glucosidase (homology mode): (a) **3a** in the electrostatics active pocket; (b) **3a** in the active pocket; (c) 3D view of **3a** with α -glucosidase; (d) 2D view of **3a** with α -glucosidase.

2.3. Inhibitory effect of OA derivatives against α -amylase

2.3.1 α -Amylase inhibition assay and SAR analysis

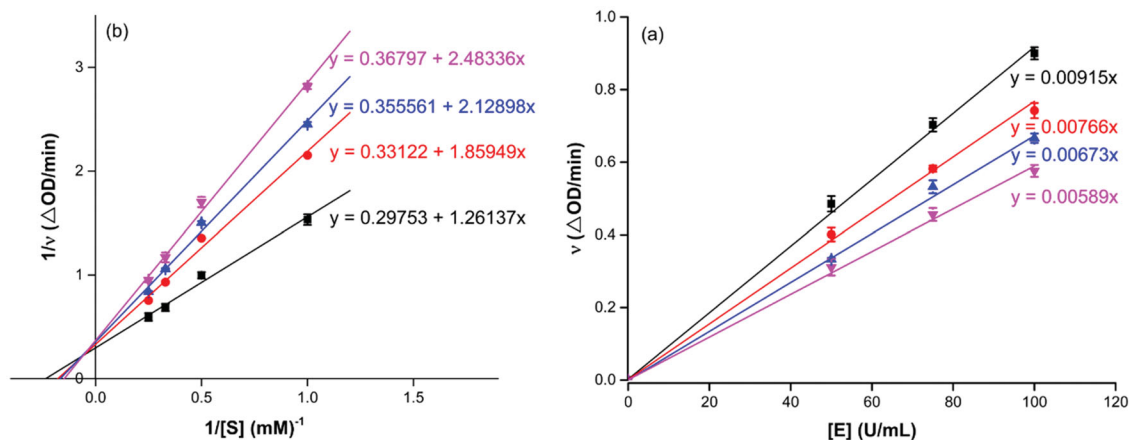
The inhibitory activities of OA derivatives against α -amylase were also tested (Table 1). All candidate compounds had potent inhibitory activities towards α -amylase with IC_{50} values ranging from 3.80 to 152.36 μ M. OA derivatives showed higher inhibitory activities than OA ($IC_{50} = 94.10 \mu$ M) and acarbose ($IC_{50} = 100.01 \mu$ M)

except compound **3t**. Among them, compound **3f** had the strongest inhibitory activity, ~ 25 times better than OA and ~ 26 times better than acarbose. Hence, it was an effective way to increase the inhibitory activities of OA against α -amylase by embedding the cinnamoyloxymino moiety into the OA motif.

For SAR analysis, it could be found that the introduction of chloro or bromo group at C4 position of benzene ring belonging

Table 2. The physicochemical properties of compounds **3a** and **3f**.

	Molecular formula	Molecular weight	Rotatable bonds	H-bond acceptor atoms	H-bond donor atoms	Polar surface area (Å ²)	LogP _{o/w}	Water solubility
3a	C ₃₉ H ₅₃ NO ₄	599.84	5	5	1	75.96	7.82	Poorly soluble
3f	C ₃₉ H ₅₂ BrNO ₄	678.74	5	5	1	75.96	8.49	Insoluble

**Figure 3.** Inhibition kinetics of **3f** against α -glucosidase. (a) The plots of enzymatic reaction rate vs α -glucosidase concentration with or without the presence of **3f**; (b) Lineweaver–Burk plots of enzymatic reaction rate vs substrate concentration with or without the presence of **3f** (**3f** concentration: black line, 0 μ M; red line, 5 μ M; blue line, 7.5 μ M; pink line, 15.0 μ M).

to the cinnamoyl group could improve the inhibitory activity against α -amylase of OA derivatives (compounds **3e** and **3f**). But when substituents such as methyl, methoxyl, fluoro, trifluoromethyl, nitro, methylenedioxy or hydroxyl installed into C4 position of benzene ring, the inhibitory activity against α -amylase of OA derivatives had decreased. In addition, that the icinnamoyloxymino substructure was merged with the OA parent structure (compounds **3a–3j**) had positive effect on the improvement of anti- α -amylase activity.

2.3.2. Inhibitory kinetic analysis

Compound **3f** with the strongest inhibitory activity against α -amylase was selected as the representative compound for the enzyme inhibitory kinetic analysis. As shown in Figure 3, the plots of V vs. α -amylase concentration with or without the presence of compound **3f** all passed through the origin (Figure 3(a)) and the Lineweaver–Burk plots of $1/V$ vs. $1/[S]$ with or without the presence of compound **3f** intersected in the second quadrant (Figure 3(b)). The results indicated compound **3f** was reversible and mixed-type inhibitor.

2.3.3. Docking simulation for α -amylase

The docking simulation results between compound **3f** and α -amylase were shown in Figure 4. It was observed that OA part of compound **3f** located into the active site of α -amylase and cinnamic acid part located near the edge of the active site (Figure 4(a,b)). The carboxylic oxygen at OA part formed a hydrogen bond with His305 (1.9 Å), and hydrophobic interaction with Trp59, Leu162, Val163, Leu165, Tyr151, Lys200, His201, and Ile235. The binding affinity of compound **3f** regarding α -amylase was -2.1 kcal/mol. The physicochemical properties of **3f** was also shown in Table 2.

2.4. Cells cytotoxicity assay

The preliminary *in vitro* cells cytotoxicity of most potent compounds **3a** and **3f** were evaluated against 3T3-L1 and HepG2 using MTT method. Compounds **3a** and **3f** had non-cytotoxic to 3T3-L1 and HepG2 cells under concentration of 100 μ M (Figure 5), indicating that the compounds had a high level of safety profile.

3. Conclusion

In summary, OA oxime ester derivatives (**3a–3f**) were synthesised and evaluated for inhibitory activities against α -glucosidase and α -amylase. All the synthesised OA derivatives had potent inhibitory activities against α -glucosidase and α -amylase. The introduction of cinnamoyloxymino moiety into the OA parent structure had better α -glucosidase and α -amylase inhibitory activities than that of benzoyloxymino moiety. Compound **3a** had highest inhibitory activity against α -glucosidase with IC₅₀ value of 0.35 μ M, \sim 1900 times stronger than acarbose, meanwhile compound **3f** had the highest α -amylase inhibitory activity with IC₅₀ value of 3.80 μ M, \sim 26 times higher than acarbose. Furthermore, the inhibition kinetic studies and docking simulation indicated the binding between compounds with protein and the low toxicity against 3T3-L1 and HepG2 cells provided the foundation for further *in vivo* assay. Considering all these experimental data, OA oxime ester derivatives could be developed into the leading compound in the management of T2D.

4. Experimental

4.1. Materials and methods

α -Glucosidase from *Saccharomyces cerevisiae* (EC 3.2.1.20), α -amylase from hog pancreas (EC3.2.1.1), *p*-Nitrophenyl- α -D-galactopyranoside (*p*-NPG). Water-soluble starch was obtained from Shanghai Yuanye Biological Technology Co., Ltd. OA was purchased from

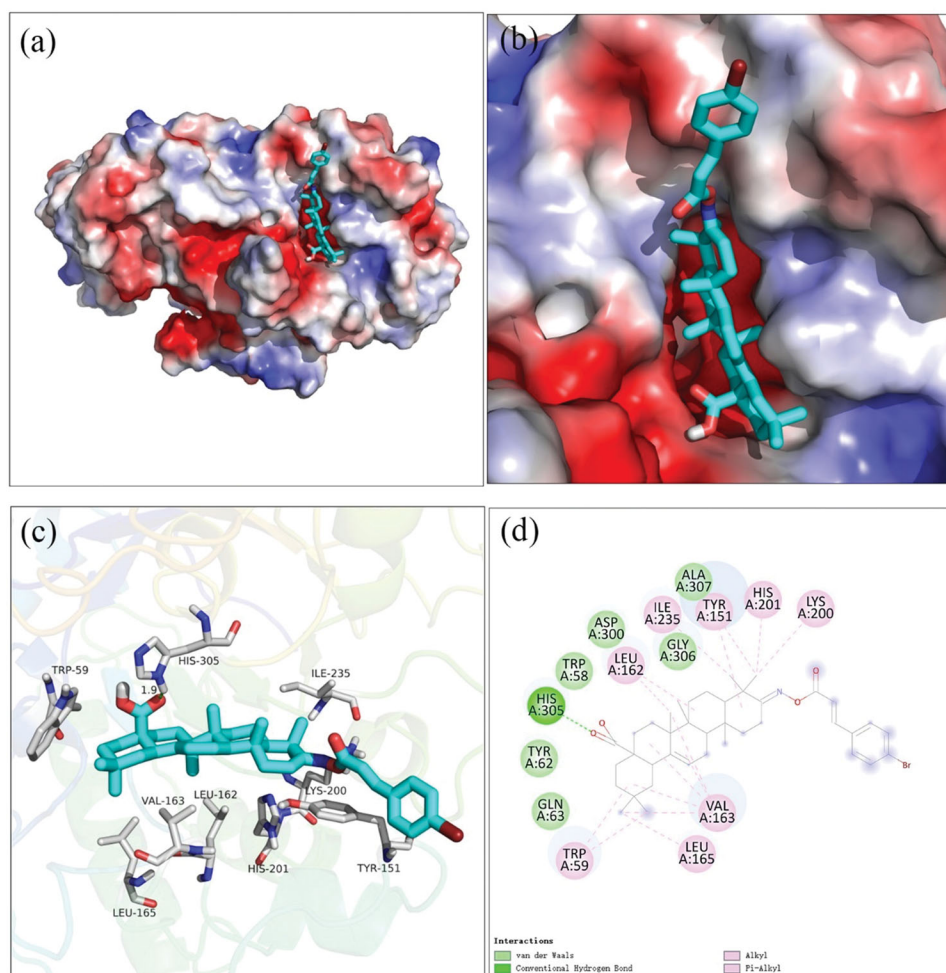


Figure 4. The molecular docking of analogue 3f and α -amylase (3BAJ): (a) 3f in the electrostatics active pocket; (b) 3f in the active pocket; (c) 3D view of 3f and α -amylase; (d) 2D view of 3f and α -amylase.

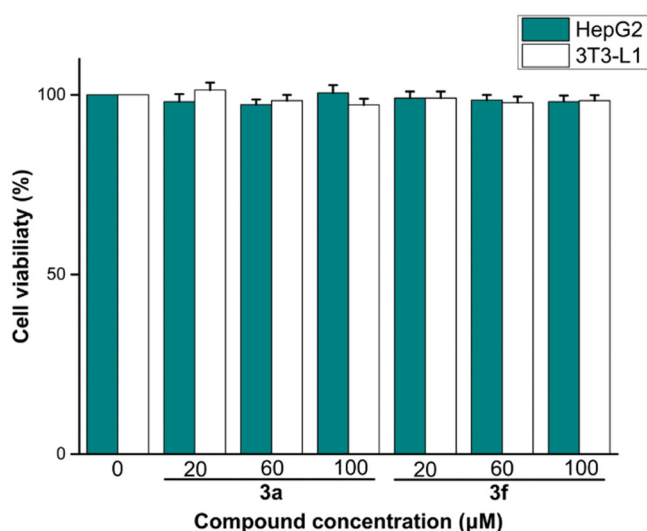


Figure 5. Cells cytotoxicity of compounds 3a and 3f against 3T3-L1 and HepG2 cells.

Macklin Co., Ltd. Other chemical reagents were obtained from Titan (Shanghai) Technology Co., Ltd. 3T3-L1 cells and HepG2 cells were supplied by ATCC. 3-(4,5-Dimethylthiazol-2-yl)-2,5-diphenyl-tetrazoliumbromide (MTT) were supported by Sigma-Aldrich.

Dulbecco's Modified Eagle's Medium (DMEM), Foetal bovine serum (FBS), penicillin and streptomycin were obtained from Gibco.

^1H NMR and ^{13}C NMR spectra were recorded in CDCl_3 on 500 MHz instruments. High-resolution mass spectral analysis (HRMS) data were measured on the Apex II by means of the ESI technique.

4.2. Synthesis of OA derivatives 3a–3t

To a solution of oleanolic acid (1.0 mmol) in acetone (10 ml), freshly Jones reagent was added dropwise in an ice bath. The reaction mixture allowed to warm to room temperature and stirred for 4 h. Firstly, MeOH was added and then water to the reaction mixture. The organic solvent was removed under vacuum and the aqueous residue was extracted with EtOAc. The organic phase was washed with water and brine, dried by MgSO_4 and evaporated under vacuum. Then, the crude product was purified by silica gel column chromatograph to obtain compound 1.

Subsequently, to a solution of $\text{NH}_2\text{OH}\cdot\text{HCl}$ (1.5 mmol) in ethanol (10 ml) was added NaOAc (2.0 mmol) and the mixture was stirred for 15 min at room temperature. Compound 1 was added to the reaction mixture and the mixture was stirred for 24 h at 50°C . After ethanol was removed under vacuum, the residue was treated with water and filtrated to afford compound 2.

Finally, freshly prepared substituted cinnamoyl chloride or benzoyl chloride (1.2 mmol) was added into the solution of compound

2 (1.0 mmol) and pyridine in DCM at 0°C, and then, the mixture was stirred at room temperature until completion. The reaction was quenched with saturated NaHCO₃ and extracted by EtOAc. The organic phase was washed with water and brine, dried by MgSO₄ and removed under vacuum to obtain the residue followed by purification through silica gel column chromatograph to produce the corresponding oleanolic acid oxime ester derivatives **3a–3t**.

8a (C₃₉H₅₃NO₄). White powder; Yield 68%. ¹H NMR (500 MHz, Chloroform-*d*) δ 7.78 (d, *J* = 16.0 Hz, 1H), 7.55 (dt, *J* = 6.7, 3.9 Hz, 2H), 7.42–7.36 (*m*, 3H), 6.58 (d, *J* = 16.0 Hz, 1H), 5.29 (t, *J* = 3.7 Hz, 1H), 3.07–2.99 (*m*, 1H), 2.86–2.79 (*m*, 1H), 2.37 (ddd, *J* = 15.0, 12.2, 5.8 Hz, 1H), 1.97 (qd, *J* = 15.6, 14.7, 3.6 Hz, 2H), 1.91–1.82 (*m*, 1H), 1.82–1.66 (*m*, 3H), 1.64–1.55 (*m*, 5H), 1.51–1.42 (*m*, 2H), 1.35 (*s*, 2H), 1.32 (*s*, 3H), 1.24 (d, *J* = 10.0 Hz, 1H), 1.22–1.07 (*m*, 9H), 1.05 (*s*, 3H), 0.91 (d, *J* = 12.2 Hz, 7H), 0.80 (*s*, 3H). ¹³C NMR (126 MHz, Chloroform-*d*) δ 183.51, 175.45, 165.31, 145.48, 143.77, 134.48, 130.46, 128.94, 128.20, 122.33, 116.35, 55.86, 47.18, 46.57, 45.81, 41.71, 41.53, 41.02, 39.33, 38.75, 37.07, 33.79, 33.07, 32.36 (d, *J* = 9.5 Hz), 30.69, 27.64, 27.09, 25.88, 23.53 (d, *J* = 13.2 Hz), 23.16, 22.91, 19.64, 18.95, 17.07, 15.16. HRMS (ESI-MS) *m/z*: [M + H]⁺ calcd for C₃₉H₅₃NO₄: 600.4047; found: 600.4026.

8b (C₄₀H₅₅NO₄). White powder; Yield 60%. ¹H NMR (500 MHz, Chloroform-*d*) δ 7.75 (d, *J* = 16.0 Hz, 1H), 7.45 (d, *J* = 7.9 Hz, 2H), 7.20 (d, *J* = 7.8 Hz, 2H), 6.53 (d, *J* = 16.0 Hz, 1H), 5.29 (t, *J* = 3.7 Hz, 1H), 3.03 (dt, *J* = 15.2, 4.5 Hz, 1H), 2.82 (dd, *J* = 14.0, 4.6 Hz, 1H), 2.38 (*s*, 4H), 2.42–2.32 (*m*, 1H), 2.03–1.82 (*m*, 4H), 1.82–1.72 (*m*, 2H), 1.72–1.55 (*m*, 5H), 1.47 (ddt, *J* = 18.4, 13.5, 7.8 Hz, 2H), 1.35 (ddd, *J* = 13.0, 9.0, 3.2 Hz, 3H), 1.30–1.21 (*m*, 2H), 1.21–1.07 (*m*, 9H), 1.05 (*s*, 3H), 0.99–0.85 (*m*, 7H), 0.80 (*s*, 3H). ¹³C NMR (126 MHz, Chloroform-*d*) δ 183.36, 175.33, 165.51, 145.50, 143.77, 140.92, 131.75, 129.67, 128.20, 122.33, 115.21, 55.86, 47.17, 46.56, 45.82, 41.72, 41.52, 41.03, 39.33, 38.75, 37.07, 33.80, 33.08, 32.37 (d, *J* = 9.1 Hz), 30.69, 27.64, 27.09, 25.88, 23.53 (d, *J* = 13.5 Hz), 23.17, 22.92, 21.53, 19.62, 18.95, 17.06, 15.16. HRMS (ESI-MS) *m/z*: [M + K]⁺ calcd for C₄₀H₅₅NO₄: 652.3763; found: 652.3740.

8c (C₄₀H₅₅NO₅). White powder; Yield 70%. ¹H NMR (500 MHz, Chloroform-*d*) δ 7.73 (d, *J* = 15.9 Hz, 1H), 7.54–7.47 (*m*, 2H), 6.94–6.88 (*m*, 2H), 6.44 (d, *J* = 15.9 Hz, 1H), 5.29 (t, *J* = 3.7 Hz, 1H), 3.84 (*s*, 3H), 3.03 (ddd, *J* = 15.2, 5.2, 3.6 Hz, 1H), 2.82 (dd, *J* = 14.2, 4.6 Hz, 1H), 2.36 (ddd, *J* = 15.2, 12.3, 5.9 Hz, 1H), 2.00 (dd, *J* = 13.4, 3.8 Hz, 1H), 1.98–1.91 (*m*, 1H), 1.87 (ddd, *J* = 18.3, 6.8, 4.1 Hz, 1H), 1.82–1.66 (*m*, 3H), 1.66–1.54 (*m*, 3H), 1.51–1.41 (*m*, 2H), 1.44–1.31 (*m*, 3H), 1.31 (*s*, 3H), 1.26 (*s*, 2H), 1.22 (d, *J* = 29.2 Hz, 2H), 1.16 (*s*, 3H), 1.12 (d, *J* = 2.5 Hz, 4H), 1.05 (*s*, 3H), 0.91 (d, *J* = 12.2 Hz, 7H), 0.80 (*s*, 3H). ¹³C NMR (126 MHz, Chloroform-*d*) δ 183.23, 175.21, 165.70, 161.51, 145.17, 143.77, 129.89, 127.24, 122.34, 114.35, 113.71, 113.47, 55.86, 55.43, 47.17, 46.55, 45.81, 41.72, 41.50, 41.03, 39.32, 37.07, 33.79, 33.07, 32.36 (d, *J* = 8.5 Hz), 30.69, 27.64, 27.08, 25.87, 23.53 (d, *J* = 13.0 Hz), 23.16, 19.60, 18.94, 17.06, 15.15. HRMS (ESI-MS) *m/z*: [M + H]⁺ calcd for C₄₀H₅₅NO₅: 630.4153; found: 630.4124.

8d (C₃₉H₅₂FNO₄). Light yellow powder; Yield 55%. ¹H NMR (500 MHz, Chloroform-*d*) δ 7.73 (d, *J* = 15.9 Hz, 1H), 7.54 (dd, *J* = 8.5, 5.4 Hz, 2H), 7.08 (t, *J* = 8.4 Hz, 2H), 6.50 (d, *J* = 15.9 Hz, 1H), 5.29 (d, *J* = 3.6 Hz, 1H), 3.02 (dt, *J* = 15.3, 4.6 Hz, 1H), 2.82 (dd, *J* = 13.9, 4.6 Hz, 1H), 2.37 (ddd, *J* = 15.0, 12.2, 5.8 Hz, 1H), 2.02–1.91 (*m*, 2H), 1.87 (ddd, *J* = 18.5, 6.7, 4.0 Hz, 1H), 1.74 (dtd, *J* = 27.9, 13.6, 4.4 Hz, 3H), 1.59 (dd, *J* = 15.2, 10.1 Hz, 5H), 1.47 (ddt, *J* = 18.0, 13.3, 7.5 Hz, 2H), 1.35 (q, *J* = 5.2 Hz, 2H), 1.31 (*s*, 3H), 1.24 (dd, *J* = 11.7, 4.4 Hz, 1H), 1.21–1.07 (*m*, 9H), 1.05 (*s*, 3H), 0.91 (d, *J* = 12.1 Hz, 7H), 0.79 (*s*, 3H). ¹³C NMR (126 MHz, Chloroform-*d*) δ 183.59, 175.51, 165.10 (d, *J* = 25.8 Hz), 144.18, 143.79, 130.73 (d,

J = 3.6 Hz), 130.09 (d, *J* = 8.3 Hz), 122.31, 116.19, 116.05 (d, *J* = 8.7 Hz), 55.85, 47.17, 46.56, 45.81, 41.71, 41.54, 41.01, 39.32, 38.74, 37.07, 33.78, 33.07, 32.36 (d, *J* = 10.7 Hz), 30.69, 27.64, 27.09, 25.88, 23.53 (d, *J* = 13.0 Hz), 23.02 (d, *J* = 31.5 Hz), 19.65, 18.94, 17.07, 15.16. HRMS (ESI-MS) *m/z*: [M + Na]⁺ calcd for C₃₉H₅₂FNO₄: 640.3773; found: 640.3751.

8e (C₃₉H₅₂ClNO₄). Yellow powder; Yield 63%. ¹H NMR (500 MHz, Chloroform-*d*) δ 7.71 (d, *J* = 16.0 Hz, 1H), 7.48 (d, *J* = 8.2 Hz, 2H), 7.36 (d, *J* = 8.2 Hz, 2H), 6.54 (d, *J* = 16.0 Hz, 1H), 5.28 (t, *J* = 3.7 Hz, 1H), 3.01 (dt, *J* = 15.1, 4.5 Hz, 1H), 2.82 (dd, *J* = 13.9, 4.6 Hz, 1H), 2.37 (ddd, *J* = 15.0, 12.2, 5.8 Hz, 1H), 2.03–1.90 (*m*, 2H), 1.86 (ddd, *J* = 18.4, 6.7, 4.0 Hz, 1H), 1.76 (ddd, *J* = 14.1, 9.5, 4.6 Hz, 2H), 1.69 (dd, *J* = 13.8, 4.2 Hz, 1H), 1.59 (ddd, *J* = 17.3, 9.0, 3.6 Hz, 5H), 1.46 (dd, *J* = 10.6, 6.5 Hz, 2H), 1.33 (d, *J* = 18.7 Hz, 6H), 1.24 (d, *J* = 11.1 Hz, 1H), 1.14 (d, *J* = 17.7 Hz, 8H), 1.05 (*s*, 3H), 0.91 (d, *J* = 12.0 Hz, 7H), 0.79 (*s*, 3H). ¹³C NMR (126 MHz, Chloroform-*d*) δ 184.19, 175.57, 165.07, 143.91 (d, *J* = 29.5 Hz), 136.36, 132.95, 129.29 (d, *J* = 17.5 Hz), 122.29, 116.93, 55.84, 47.17, 46.58, 45.81, 41.62 (d, *J* = 17.7 Hz), 40.97, 39.32, 38.73, 37.07, 33.78, 33.08, 32.35 (d, *J* = 13.0 Hz), 30.69, 29.71 (d, *J* = 5.6 Hz), 27.64, 27.09, 25.89, 23.53 (d, *J* = 14.7 Hz), 23.14, 22.87, 19.65, 18.94, 17.07, 15.16. HRMS (ESI-MS) *m/z*: [M + Na]⁺ calcd for C₃₉H₅₂ClNO₄: 656.3477; found: 656.3451.

8f (C₃₉H₅₂BrNO₄). White powder; Yield 42%. ¹H NMR (500 MHz, Chloroform-*d*) δ 7.70 (d, *J* = 16.0 Hz, 1H), 7.53 (dd, *J* = 8.7, 2.4 Hz, 2H), 7.46–7.39 (*m*, 2H), 6.56 (d, *J* = 16.0 Hz, 1H), 5.29 (d, *J* = 3.6 Hz, 1H), 3.01 (dt, *J* = 15.1, 4.6 Hz, 1H), 2.82 (dd, *J* = 14.3, 4.9 Hz, 1H), 2.37 (ddd, *J* = 14.8, 12.2, 5.8 Hz, 1H), 2.03–1.91 (*m*, 2H), 1.86 (ddd, *J* = 18.4, 6.5, 3.9 Hz, 1H), 1.81–1.66 (*m*, 3H), 1.60 (qd, *J* = 11.9, 10.6, 5.5 Hz, 5H), 1.47 (dd, *J* = 10.1, 5.7 Hz, 1H), 1.43–1.33 (*m*, 3H), 1.31 (d, *J* = 5.1 Hz, 3H), 1.26 (d, *J* = 15.7 Hz, 1H), 1.24–1.18 (*m*, 1H), 1.16 (d, *J* = 3.5 Hz, 5H), 1.12 (*s*, 3H), 1.05 (*s*, 3H), 0.97 (d, *J* = 7.7 Hz, 1H), 0.91 (d, *J* = 12.2 Hz, 6H), 0.80 (d, *J* = 3.6 Hz, 3H). ¹³C NMR (126 MHz, Chloroform-*d*) δ 182.97, 175.63, 165.06, 144.10, 143.80, 133.37, 132.19, 124.72, 122.30, 117.05, 55.84, 47.17, 46.55, 45.82, 41.73, 41.55, 41.05, 39.32, 38.74, 37.07, 33.79, 33.07, 32.39, 30.69, 27.64, 27.09, 25.87, 23.53 (d, *J* = 13.0 Hz), 23.15, 22.92, 19.66, 18.95, 17.05, 15.16. HRMS (ESI-MS) *m/z*: [M + H]⁺ calcd for C₃₉H₅₂BrNO₄: 678.3152; found: 678.3130.

8g (C₄₀H₅₂F₃NO₄). White powder; Yield 46%. ¹H NMR (500 MHz, Chloroform-*d*) δ 7.78 (dd, *J* = 16.0, 1.6 Hz, 1H), 7.65 (d, *J* = 1.5 Hz, 4H), 6.64 (dd, *J* = 16.0, 1.6 Hz, 1H), 5.29 (*s*, 1H), 3.02 (dd, *J* = 15.4, 4.7 Hz, 1H), 2.83 (dd, *J* = 13.9, 4.6 Hz, 1H), 2.44–2.33 (*m*, 1H), 1.97 (dt, *J* = 18.5, 12.1 Hz, 3H), 1.91–1.84 (*m*, 1H), 1.74 (ddt, *J* = 31.2, 16.6, 8.3 Hz, 3H), 1.60 (dd, *J* = 9.9, 5.4 Hz, 5H), 1.53–1.41 (*m*, 2H), 1.33 (d, *J* = 12.7 Hz, 6H), 1.17 (*s*, 4H), 1.13 (*s*, 3H), 1.05 (*s*, 3H), 0.99–0.85 (*m*, 7H), 0.80 (*s*, 3H). ¹³C NMR (126 MHz, Chloroform-*d*) δ 205.76, 184.26, 178.48, 175.78, 174.94, 164.65 (d, *J* = 20.9 Hz), 143.69 (d, *J* = 30.1 Hz), 137.79, 132.10–131.47 (*m*), 128.33 (d, *J* = 3.2 Hz), 125.91 (t, *J* = 3.8 Hz), 124.91, 122.74, 122.25, 118.98, 118.81, 91.03, 55.82, 55.33, 50.68, 47.17, 46.56, 45.81, 44.10, 43.97, 43.71, 42.50, 41.65 (d, *J* = 4.8 Hz), 41.56, 40.95, 39.31, 38.73 (d, *J* = 5.2 Hz), 37.50, 37.29, 37.06, 34.12, 33.78, 33.12 (d, *J* = 13.8 Hz), 32.53–32.23 (*m*), 31.58, 30.68, 27.63, 27.28–26.91 (*m*), 25.86 (d, *J* = 4.1 Hz), 23.77, 23.52 (d, *J* = 15.0 Hz), 23.13, 22.82 (d, *J* = 8.4 Hz), 20.65, 19.60 (d, *J* = 20.3 Hz), 18.93, 18.36, 18.09 (d, *J* = 13.2 Hz), 17.07, 15.70, 15.14. HRMS (ESI-MS) *m/z*: [M + K]⁺ calcd for C₄₀H₅₂F₃NO₄: 706.3480; found: 706.3448.

8h (C₃₉H₅₂N₂O₆). Yellow powder; Yield 55%. ¹H NMR (500 MHz, Chloroform-*d*) δ 8.29–8.23 (*m*, 2H), 7.79 (d, *J* = 16.0 Hz, 1H), 7.70 (dd, *J* = 8.9, 2.7 Hz, 2H), 6.73–6.64 (*m*, 1H), 5.30–5.25 (*m*, 1H), 3.00 (dt, *J* = 15.1, 4.7 Hz, 1H), 2.82 (dd, *J* = 13.8, 4.6 Hz, 1H), 2.39 (ddd, *J* = 15.3, 12.3, 6.0 Hz, 1H), 2.02–1.91 (*m*, 2H), 1.89–1.76 (*m*,

1H), 1.75–1.66 (*m*, 1H), 1.64–1.55 (*m*, 6H), 1.47 (dd, *J* = 10.5, 6.1 Hz, 1H), 1.44–1.29 (*m*, 7H), 1.26 (d, *J* = 16.3 Hz, 2H), 1.17 (d, *J* = 12.8 Hz, 5H), 1.12 (*s*, 3H), 1.05 (*s*, 3H), 1.01–0.94 (*m*, 1H), 0.91 (d, *J* = 12.0 Hz, 6H), 0.79 (*s*, 3H). ¹³C NMR (126 MHz, Chloroform-*d*) δ 184.08, 176.01, 164.35, 148.58, 143.82, 142.46, 140.53, 128.78, 124.22, 122.25, 120.76, 55.83, 47.18, 46.57, 45.82, 41.65 (d, *J* = 11.1 Hz), 40.98, 39.32, 38.73, 37.07, 33.78, 33.07, 32.34 (d, *J* = 13.2 Hz), 30.69, 29.72, 27.63, 27.12, 25.88, 23.52 (d, *J* = 13.8 Hz), 23.13, 22.87, 19.73, 18.95, 17.06, 15.17. HRMS (ESI-MS) *m/z*: [M + Na]⁺ calcd for C₃₉H₅₂N₂O₆: 667.3718; found: 667.3717.

8i (C₄₀H₅₃NO₆). White powder; Yield 45%. ¹H NMR (500 MHz, Chloroform-*d*) δ 7.68 (d, *J* = 15.9 Hz, 1H), 7.09–7.00 (*m*, 2H), 6.82 (d, *J* = 8.1 Hz, 1H), 6.40 (d, *J* = 15.9 Hz, 1H), 6.01 (*s*, 2H), 5.28 (t, *J* = 3.6 Hz, 1H), 3.02 (dt, *J* = 15.1, 4.5 Hz, 1H), 2.82 (dd, *J* = 13.7, 4.7 Hz, 1H), 2.36 (ddd, *J* = 15.1, 12.3, 6.1 Hz, 1H), 1.97 (qd, *J* = 15.2, 14.4, 3.6 Hz, 2H), 1.86 (ddd, *J* = 18.5, 6.5, 3.8 Hz, 1H), 1.81–1.66 (*m*, 3H), 1.61–1.55 (*m*, 1H), 1.53–1.45 (*m*, 1H), 1.44–1.34 (*m*, 1H), 1.37–1.24 (*m*, 9H), 1.16 (d, *J* = 5.5 Hz, 7H), 1.12 (*s*, 3H), 1.05 (*s*, 3H), 0.91 (d, *J* = 12.3 Hz, 7H), 0.79 (*s*, 3H). ¹³C NMR (126 MHz, Chloroform-*d*) δ 183.61, 175.29, 165.57, 149.75, 148.38, 145.22, 143.77, 128.93, 124.72, 122.33, 114.16, 108.59, 106.54, 101.62, 55.85, 47.17, 46.57, 45.81, 41.71, 41.51, 41.02, 39.32, 38.74, 37.07, 33.79, 33.08, 32.36 (d, *J* = 9.9 Hz), 30.69, 29.73, 27.63, 27.08, 25.88, 23.53 (d, *J* = 14.0 Hz), 23.03 (d, *J* = 31.3 Hz), 19.61, 18.94, 17.04, 15.15. HRMS (ESI-MS) *m/z*: [M + Na]⁺ calcd for C₄₀H₅₃NO₆: 666.3765; found: 666.3736.

8j (C₃₉H₅₃NO₅). White powder; Yield 40%. ¹H NMR (500 MHz, Chloroform-*d*) δ 7.73 (d, *J* = 15.9 Hz, 1H), 7.43 (d, *J* = 8.3 Hz, 2H), 6.89 (d, *J* = 8.3 Hz, 2H), 6.42 (d, *J* = 15.9 Hz, 1H), 5.27 (d, *J* = 3.8 Hz, 1H), 2.99 (dt, *J* = 15.3, 4.8 Hz, 1H), 2.82 (dd, *J* = 13.9, 4.6 Hz, 1H), 2.40 (ddd, *J* = 15.3, 12.1, 6.2 Hz, 1H), 2.03–1.82 (*m*, 3H), 1.73 (ddt, *J* = 25.4, 15.8, 8.4 Hz, 3H), 1.60 (*q*, *J* = 11.3, 9.5 Hz, 6H), 1.50–1.29 (*m*, 3H), 1.28–1.06 (*m*, 12H), 1.02 (*s*, 3H), 0.98–0.86 (*m*, 8H), 0.77 (*s*, 3H). ¹³C NMR (126 MHz, Chloroform-*d*) δ 184.23, 175.58, 166.74, 158.90, 146.21, 143.74, 130.19, 126.56, 122.37, 116.16, 112.68, 55.62, 47.11, 46.59, 45.78, 41.67, 41.46, 40.99, 39.30, 38.59, 37.04, 33.77, 33.09, 32.34 (d, *J* = 23.0 Hz), 30.69, 27.63, 27.19, 25.90, 23.52 (d, *J* = 16.9 Hz), 22.98 (d, *J* = 32.1 Hz), 19.70, 18.96, 17.09, 15.18. HRMS (ESI-MS) *m/z*: [M + K]⁺ calcd for C₃₉H₅₃NO₅: 654.3555; found: 654.3525.

8k (C₃₇H₅₁NO₄). White powder; Yield 70%. ¹H NMR (500 MHz, Chloroform-*d*) δ 8.08–8.03 (*m*, 2H), 7.58 (td, *J* = 7.3, 1.3 Hz, 1H), 7.46 (t, *J* = 7.8 Hz, 2H), 5.29 (d, *J* = 3.8 Hz, 1H), 3.11–3.03 (*m*, 1H), 2.83 (dd, *J* = 13.9, 4.6 Hz, 1H), 2.44 (ddd, *J* = 15.2, 12.2, 5.9 Hz, 1H), 1.97 (qd, *J* = 14.9, 14.2, 3.6 Hz, 2H), 1.90–1.82 (*m*, 1H), 1.75 (ddt, *J* = 28.0, 13.9, 4.9 Hz, 3H), 1.62 (td, *J* = 12.2, 10.2, 5.1 Hz, 5H), 1.54–1.44 (*m*, 2H), 1.35 (*s*, 6H), 1.26–1.20 (*m*, 3H), 1.13 (d, *J* = 5.3 Hz, 5H), 1.07 (*s*, 3H), 0.91 (d, *J* = 12.1 Hz, 7H), 0.81 (*s*, 3H). ¹³C NMR (126 MHz, Chloroform-*d*) δ 183.76, 176.24, 164.32, 143.78, 133.04, 129.54, 128.50, 122.31, 55.82, 47.16, 46.58, 45.80, 41.67 (d, *J* = 10.9 Hz), 41.01, 39.33, 38.74, 37.09, 33.79, 33.07, 32.36 (d, *J* = 10.6 Hz), 30.69, 27.64, 27.14, 25.89, 23.53 (d, *J* = 13.9 Hz), 23.21, 22.89, 19.88, 18.95, 17.07, 15.16. HRMS (ESI-MS) *m/z*: [M + K]⁺ calcd for C₃₇H₅₁NO₄: 612.3450; found: 612.3423.

8l (C₃₈H₅₃NO₄). White powder; Yield 68%. ¹H NMR (500 MHz, Chloroform-*d*) δ 7.93 (d, *J* = 8.1 Hz, 2H), 7.23 (d, *J* = 8.0 Hz, 2H), 5.26 (d, *J* = 3.9 Hz, 1H), 3.06 (dt, *J* = 15.3, 4.6 Hz, 1H), 2.82 (dd, *J* = 14.0, 4.6 Hz, 1H), 2.40 (*s*, 4H), 2.01–1.90 (*m*, 2H), 1.90–1.81 (*m*, 1H), 1.74 (tdd, *J* = 20.0, 18.2, 9.8, 3.9 Hz, 3H), 1.59 (td, *J* = 17.0, 14.9, 8.6 Hz, 5H), 1.51–1.40 (*m*, 2H), 1.34 (*s*, 5H), 1.24 (*s*, 1H), 1.18 (d, *J* = 5.2 Hz, 5H), 1.11 (*s*, 4H), 1.05 (*s*, 3H), 0.90 (d, *J* = 12.3 Hz, 7H), 0.79 (*s*, 3H). ¹³C NMR (126 MHz, Chloroform-*d*) δ 184.64, 176.00, 164.39, 143.76 (d, *J* = 5.5 Hz), 129.57, 129.22, 126.86, 122.30, 55.81,

47.15, 46.58, 45.80, 41.63 (d, *J* = 10.8 Hz), 40.95, 39.32, 38.71, 37.08, 33.79, 33.10, 32.36 (d, *J* = 14.3 Hz), 30.68, 27.63, 27.15, 25.91, 23.53 (d, *J* = 17.4 Hz), 23.22, 22.86, 21.75, 19.85, 18.94, 17.07, 15.14. HRMS (ESI-MS) *m/z*: [M + H]⁺ calcd for C₃₈H₅₃NO₄: 588.4047; found: 588.4018.

8m (C₃₈H₅₃NO₅). Yellow powder; Yield 44%. ¹H NMR (500 MHz, Chloroform-*d*) δ 8.07–7.97 (*m*, 2H), 6.94 (dd, *J* = 9.2, 2.4 Hz, 2H), 5.28 (t, *J* = 3.7 Hz, 1H), 3.87 (*s*, 3H), 3.11–3.02 (*m*, 1H), 2.82 (dd, *J* = 14.0, 4.6 Hz, 1H), 2.47–2.35 (*m*, 1H), 2.03–1.83 (*m*, 3H), 1.81–1.70 (*m*, 3H), 1.62 (ddd, *J* = 12.7, 9.6, 5.1 Hz, 5H), 1.51–1.30 (*m*, 8H), 1.25 (d, *J* = 2.2 Hz, 2H), 1.19–1.10 (*m*, 7H), 1.06 (*s*, 3H), 0.92 (dd, *J* = 11.1, 5.3 Hz, 7H), 0.80 (*s*, 3H). ¹³C NMR (126 MHz, Chloroform-*d*) δ 183.58, 175.85, 164.09, 163.42, 143.78, 131.58, 122.32, 121.96, 113.77, 55.82, 55.48, 47.15, 46.57, 45.80, 41.65 (d, *J* = 17.4 Hz), 41.02, 39.33, 38.73, 37.08, 33.79, 33.08, 32.36 (d, *J* = 9.5 Hz), 30.69, 27.63, 27.13, 25.88, 23.53 (d, *J* = 14.5 Hz), 23.22, 22.90, 19.83, 18.94, 17.07, 15.14. HRMS (ESI-MS) *m/z*: [M + H]⁺ calcd for C₃₈H₅₃NO₅: 604.3997; found: 604.3997.

8n (C₃₇H₅₀FNO₄). White powder; Yield 56%. ¹H NMR (500 MHz, Chloroform-*d*) δ 8.10–8.03 (*m*, 2H), 7.13 (t, *J* = 8.6 Hz, 2H), 5.28 (t, *J* = 3.7 Hz, 1H), 3.04 (ddd, *J* = 15.3, 5.4, 3.7 Hz, 1H), 2.82 (dd, *J* = 13.8, 4.6 Hz, 1H), 2.44 (ddd, *J* = 15.2, 12.2, 5.9 Hz, 1H), 2.03–1.91 (*m*, 2H), 1.90–1.67 (*m*, 4H), 1.65–1.55 (*m*, 5H), 1.47 (qd, *J* = 14.1, 13.2, 7.4 Hz, 2H), 1.39–1.30 (*m*, 5H), 1.27–1.20 (*m*, 2H), 1.18 (*s*, 3H), 1.17–1.09 (*m*, 4H), 1.06 (*s*, 4H), 0.91 (d, *J* = 11.9 Hz, 7H), 0.79 (*s*, 3H). ¹³C NMR (126 MHz, Chloroform-*d*) δ 184.23, 176.31, 166.81, 164.78, 163.38, 143.80, 132.07 (d, *J* = 9.2 Hz), 125.89 (d, *J* = 3.4 Hz), 122.28, 115.71 (d, *J* = 22.0 Hz), 55.79, 47.15, 46.58, 45.80, 41.67 (d, *J* = 6.6 Hz), 40.97, 39.32, 38.71, 37.08, 33.78, 33.07, 32.35 (d, *J* = 13.4 Hz), 30.69, 27.63, 27.15, 25.89, 23.52 (d, *J* = 14.7 Hz), 23.20, 22.87, 19.90, 18.94, 17.07, 15.16. HRMS (ESI-MS) *m/z*: [M + K]⁺ calcd for C₃₇H₅₀FNO₄: 630.3355; found: 630.3326.

8o (C₃₇H₅₀ClNO₄). White powder; Yield 65%. ¹H NMR (500 MHz, Chloroform-*d*) δ 8.01–7.96 (*m*, 2H), 7.46–7.40 (*m*, 2H), 5.28 (*q*, *J* = 3.9 Hz, 1H), 3.03 (ddd, *J* = 15.3, 5.4, 3.7 Hz, 1H), 2.82 (dd, *J* = 13.8, 4.7 Hz, 1H), 2.43 (ddd, *J* = 15.2, 12.2, 5.9 Hz, 1H), 2.03–1.90 (*m*, 2H), 1.86 (ddd, *J* = 18.3, 6.5, 3.9 Hz, 1H), 1.82–1.67 (*m*, 3H), 1.66–1.54 (*m*, 6H), 1.53–1.42 (*m*, 2H), 1.41–1.30 (*m*, 6H), 1.29–1.20 (*m*, 2H), 1.18 (*s*, 3H), 1.12 (*s*, 3H), 1.06 (*s*, 3H), 0.91 (d, *J* = 11.9 Hz, 7H), 0.79 (*s*, 3H). ¹³C NMR (126 MHz, Chloroform-*d*) δ 184.13, 176.45, 163.49, 143.80, 139.50, 130.92, 128.89, 128.12, 122.27, 55.79, 47.15, 46.58, 45.80, 41.68 (d, *J* = 3.8 Hz), 40.98, 39.32, 38.70, 37.08, 33.78, 33.08, 32.35 (d, *J* = 13.5 Hz), 30.69, 27.63, 27.15, 25.89, 23.52 (d, *J* = 14.8 Hz), 23.20, 22.87, 19.92, 18.94, 17.07, 15.16. HRMS (ESI-MS) *m/z*: [M + H]⁺ calcd for C₃₇H₅₀ClNO₄: 608.3501; found: 608.3482.

8p (C₃₇H₅₀BrNO₄). White powder; Yield 42%. ¹H NMR (500 MHz, Chloroform-*d*) δ 7.93–7.88 (*m*, 2H), 7.62–7.56 (*m*, 2H), 5.28 (*q*, *J* = 3.8 Hz, 1H), 3.02 (ddd, *J* = 15.3, 5.3, 3.7 Hz, 1H), 2.82 (dd, *J* = 13.8, 4.6 Hz, 1H), 2.43 (ddd, *J* = 15.1, 12.1, 5.9 Hz, 1H), 2.03–1.91 (*m*, 2H), 1.86 (ddd, *J* = 18.3, 6.6, 4.0 Hz, 1H), 1.82–1.67 (*m*, 3H), 1.67–1.54 (*m*, 5H), 1.53–1.39 (*m*, 3H), 1.38–1.30 (*m*, 5H), 1.26–1.20 (*m*, 2H), 1.18 (*s*, 3H), 1.12 (*s*, 3H), 1.08 (*s*, 1H), 1.06 (*s*, 3H), 0.91 (d, *J* = 11.8 Hz, 7H), 0.79 (d, *J* = 3.6 Hz, 3H). ¹³C NMR (126 MHz, Chloroform-*d*) δ 184.26, 176.46, 163.60, 143.78, 131.86, 131.03, 128.57, 128.15, 122.26, 55.79, 47.15, 46.58, 45.80, 41.67 (d, *J* = 3.0 Hz), 40.98 (d, *J* = 4.0 Hz), 39.32, 38.70, 37.08, 33.78, 33.08, 32.34 (d, *J* = 13.8 Hz), 30.69, 27.63, 27.14, 25.89, 23.52 (d, *J* = 15.2 Hz), 23.20, 22.86, 19.93, 18.94, 17.07, 15.15. HRMS (ESI-MS) *m/z*: [M + K]⁺ calcd for C₃₇H₅₀BrNO₄: 690.2555; found: 690.2524.

8q (C₃₈H₅₀F₃NO₄). White powder; Yield 43%. ¹H NMR (500 MHz, Chloroform-*d*) δ 8.16 (d, *J* = 8.1 Hz, 2H), 7.72 (d, *J* = 8.2 Hz, 2H),

5.28 (t, $J=3.6$ Hz, 1H), 3.08–2.99 (m, 1H), 2.82 (dd, $J=13.9$, 4.6 Hz, 1H), 2.46 (ddd, $J=15.2$, 12.1, 5.9 Hz, 1H), 2.03–1.91 (m, 2H), 1.90–1.75 (m, 2H), 1.75–1.67 (m, 1H), 1.60 (ddt, $J=18.0$, 13.5, 6.8 Hz, 5H), 1.53–1.40 (m, 2H), 1.35 (s, 5H), 1.29–1.22 (m, 3H), 1.20 (s, 3H), 1.17–1.04 (m, 8H), 0.91 (d, $J=12.0$ Hz, 7H), 0.80 (s, 3H). ^{13}C NMR (126 MHz, Chloroform- d) δ 184.40, 176.83, 163.14, 143.80, 134.52 (d, $J=32.3$ Hz), 132.99, 129.93, 126.11–125.38 (m), 122.25, 55.80, 47.16, 46.59, 45.80, 41.70 (d, $J=4.6$ Hz), 40.96, 39.32, 38.70, 37.09, 33.78, 33.07, 32.34 (d, $J=14.6$ Hz), 30.69, 27.63, 27.15, 25.89, 23.52 (d, $J=14.6$ Hz), 23.19, 22.86, 19.98, 18.94, 17.07, 15.17. HRMS (ESI-MS) m/z : $[\text{M} + \text{H}]^+$ calcd for $\text{C}_{38}\text{H}_{50}\text{F}_3\text{NO}_4$: 642.3765; found: 642.3736.

8r ($\text{C}_{37}\text{H}_{50}\text{N}_2\text{O}_6$). Yellow powder; Yield 57%. ^1H NMR (500 MHz, Chloroform- d) δ 8.31 (d, $J=8.5$ Hz, 2H), 8.22 (d, $J=8.6$ Hz, 2H), 5.28 (t, $J=3.6$ Hz, 1H), 3.03 (dt, $J=15.2$, 4.7 Hz, 1H), 2.82 (dd, $J=13.8$, 4.6 Hz, 1H), 2.47 (ddd, $J=15.1$, 12.0, 6.0 Hz, 1H), 1.97 (qd, $J=11.8$, 3.3 Hz, 2H), 1.90–1.78 (m, 2H), 1.77–1.70 (m, 1H), 1.65–1.54 (m, 5H), 1.51–1.40 (m, 2H), 1.39–1.27 (m, 7H), 1.23–1.22 (m, 1H), 1.20 (s, 4H), 1.12 (s, 4H), 1.07 (d, $J=6.9$ Hz, 3H), 0.91 (d, $J=12.1$ Hz, 7H), 0.80 (s, 3H). ^{13}C NMR (126 MHz, Chloroform- d) δ 184.33, 177.14, 162.47, 150.56, 143.82, 135.19, 130.65, 123.72, 122.22, 55.78, 47.16, 46.58, 45.81, 41.73 (d, $J=10.1$ Hz), 40.96, 39.32, 38.69, 37.09, 33.78, 33.07, 32.33 (d, $J=15.3$ Hz), 30.69, 29.71 (d, $J=5.3$ Hz), 27.63, 27.18, 25.89, 23.52 (d, $J=14.7$ Hz), 23.20, 22.79 (d, $J=17.3$ Hz), 20.07, 18.95, 17.05, 15.18. HRMS (ESI-MS) m/z : $[\text{M} + \text{H}]^+$ calcd for $\text{C}_{37}\text{H}_{50}\text{N}_2\text{O}_6$: 619.3742; found: 619.3724.

8s ($\text{C}_{38}\text{H}_{51}\text{NO}_6$). White powder; Yield 44%. ^1H NMR (500 MHz, Chloroform- d) δ 7.66 (dd, $J=8.1$, 1.7 Hz, 1H), 7.48 (d, $J=1.7$ Hz, 1H), 6.86 (d, $J=8.2$ Hz, 1H), 6.05 (s, 2H), 5.29 (t, $J=3.7$ Hz, 1H), 3.04 (ddd, $J=15.3$, 5.4, 3.7 Hz, 1H), 2.83 (dd, $J=13.8$, 4.6 Hz, 1H), 2.42 (ddd, $J=15.2$, 12.2, 5.9 Hz, 1H), 2.05–1.92 (m, 2H), 1.90–1.83 (m, 1H), 1.82–1.73 (m, 2H), 1.72–1.67 (m, 1H), 1.66–1.56 (m, 6H), 1.53–1.35 (m, 3H), 1.33 (s, 3H), 1.22–1.16 (m, 5H), 1.13 (s, 4H), 1.06 (s, 4H), 0.91 (d, $J=12.1$ Hz, 7H), 0.80 (s, 3H). ^{13}C NMR (126 MHz, Chloroform- d) δ 182.65, 175.97, 163.70, 151.70, 147.79, 143.77, 125.33, 123.53, 122.33, 109.45, 108.15, 101.87, 55.82, 47.15, 46.54, 45.81, 41.74, 41.59, 41.08, 39.32, 38.73, 37.07, 33.79, 33.07, 32.36 (d, $J=7.6$ Hz), 30.70, 29.73, 27.64, 27.14, 25.87, 23.52 (d, $J=13.0$ Hz), 23.22, 22.94, 19.87, 18.96, 17.04, 15.15. HRMS (ESI-MS) m/z : $[\text{M} + \text{H}]^+$ calcd for $\text{C}_{38}\text{H}_{51}\text{NO}_6$: 618.3789; found: 618.3760.

8t ($\text{C}_{37}\text{H}_{51}\text{NO}_5$). Yellow powder; Yield 45%. ^1H NMR (500 MHz, DMSO- d_6) δ 12.07 (s, 1H), 10.41 (s, 1H), 7.87–7.81 (m, 2H), 6.91–6.84 (m, 2H), 5.20–5.15 (m, 1H), 2.96 (dt, $J=15.2$, 4.8 Hz, 1H), 2.74 (dd, $J=14.0$, 4.5 Hz, 1H), 1.96–1.81 (m, 2H), 1.69 (dd, $J=12.1$, 6.3 Hz, 1H), 1.66–1.53 (m, 3H), 1.51–1.40 (m, 4H), 1.37–1.25 (m, 3H), 1.22 (d, $J=7.4$ Hz, 7H), 1.18–1.08 (m, 9H), 0.99 (s, 3H), 0.87 (s, 7H), 0.76 (s, 3H). ^{13}C NMR (126 MHz, DMSO- d_6) δ 179.10, 175.68, 163.52, 162.63, 144.35, 131.88, 121.86, 119.84, 116.03, 55.43, 46.91, 46.02 (d, $J=17.4$ Hz), 41.90, 41.36 (d, $J=11.9$ Hz), 38.51, 37.03, 33.77, 33.29, 32.49 (d, $J=11.9$ Hz), 30.87, 27.67 (d, $J=5.7$ Hz), 25.95, 23.83, 23.43, 23.07, 19.73, 19.03, 17.22, 15.24. HRMS (ESI-MS) m/z : $[\text{M} + \text{K}]^+$ calcd for $\text{C}_{37}\text{H}_{51}\text{NO}_5$: 628.3399; found: 628.3378.

4.3. α -Glucosidase inhibition and kinetics assay

The α -glucosidase inhibition assay of all the synthesised OA derivatives (**3a–3t**) was performed according to previously reported method with minor modifications^{22–24}. Briefly, α -glucosidase (10 μL , final concentration 0.1 U/mL, dissolved in PBS), test compound (10 μL , dissolved in DMSO), and PBS (130 μL , 0.1 M phosphate, pH 6.8) were added into a 96-well plate and the mixture

was incubated at 37 °C for 10 min. After *p*-NPG (50 μL , final concentration 0.25 mM) was added, the absorbance of the mixture was measured at 405 nm at every 10 minutes using Microplate reader. DMSO working concentration in enzyme inhibition test was 5%. Acarbose was used as a positive control for α -glucosidase inhibition assay. Inhibition rate (%) = $[(A_1 - A_0)/A_0] \times 100\%$, where A_1 and A_0 represent the absorbance of the blank and test compound, respectively. IC50 value of each compound were obtained from the inhibition curve. All samples were assayed at least in triplicate.

The enzyme inhibition kinetics analysis was investigated using previously reported method with minor modifications^{25,26}. In brief, inhibitory effect was determined from the plots of absorbance change of OA derivatives at different concentrations with enzyme at different concentrations. The inhibition type was measured based on the Lineweaver–Burk plot of absorbance change of OA derivatives at different concentrations with *p*-NPG substrate at different concentrations.

4.4. α -Amylase inhibition and kinetics assay

The α -amylase inhibition of OA derivatives (**3a–3t**) was also assayed using previously reported method with minor modifications^{27–29}. Briefly, α -amylase (10 μL , final concentration 0.25 U/mL) and test compound (10 μL) were added into PBS (80 μL , 20 mM phosphate, pH 6.9) and the mixture was incubated at 37 °C for 10 min. After starch solution (100 μL , final concentration 0.5%) was added, the mixture was incubation at 37 °C for 10 min. Then DNS (100 μL , containing 1 M potassium sodium tartrate and 48 mM 3,5-Dinitrosalicylic acid) was added and the mixture was boiled for 15 min. Then, the absorbance was measured at 540 nm. The inhibition rate (%) = $[(A_1 - A_0)/A_0] \times 100\%$, where A_1 and A_0 represent the absorbance of the blank and test compound, respectively. The IC50 values of all the synthesised compounds were obtained from the inhibition curve. All samples were assayed at least in triplicate.

The enzyme inhibition kinetics analysis was investigated. The operation method was similar with the assay of α -glucosidase, except the concentrations of test compound, enzyme and substrate.

4.5. Molecular docking

Molecular docking was simulated to show the binding between inhibitor with target protein using Sybyl software (Tripos, US)²¹. The crystal structure of *Saccharomyces cerevisiae* isomaltase has not been reported, then the homology mode of α -glucosidase was constructed. The sequence in FASTA format of α -glucosidase (access code P53341) was obtained from UniProt. *Saccharomyces cerevisiae* isomaltase (PDB ID: 3AJ7) showing 72.4% of sequence identity with α -glucosidase was selected as the template^{30–32}. Then, modeller 10.1 software (<http://salilab.org/modeller/>) was used to establish homology mode and Ramachandran plot (<http://services.mbi.ucla.edu/PROCHECK/>) was used to verify their quality³³. The most reasonable homology mode (Figure 6) was used for subsequent docking experiments. The human pancreatic α -amylase (PDB: 3BAJ) were obtained from the Protein Data Bank^{34,35}. The protein was prepared following standard operating procedures and the active pocket was generated using blind or ligand mode, respectively. Compound **3a** for α -glucosidase and compound **3f** for α -amylase were respectively prepared with energy minimisation program. After that, the molecular docking of between inhibitor and target protein was operated in the default

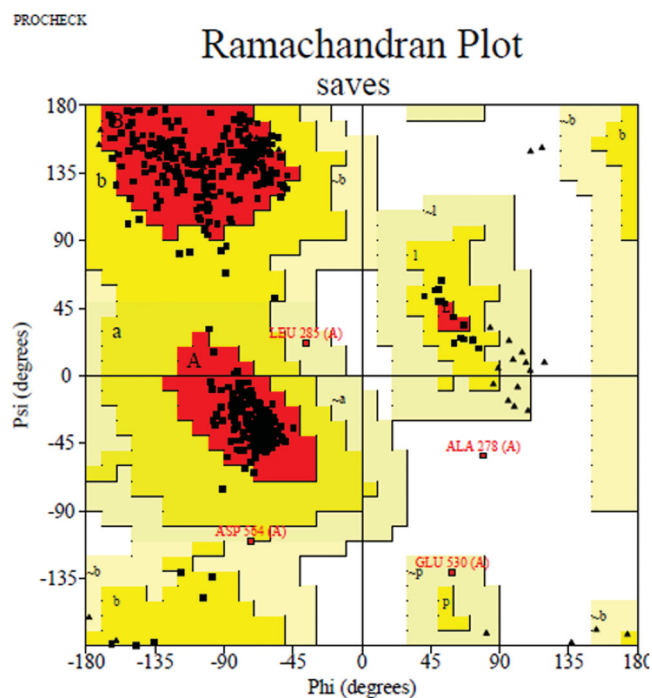


Figure 6. Ramachandran plot results of most reasonable homology mode.

format. The interactions were visualised by Pymol software and Discovery studio software.

4.6. Cells cytotoxicity assay

Cells cytotoxicity of the most potent compounds (**3a** and **3f**) on 3T3-L1 and HepG2 cells were evaluated *via* MTT method^{36,37}. 3T3-L1 or HepG2 cells were cultured in Dulbecco's modified Eagle medium (DMEM) with 10% foetal bovine serum (FBS), 100 IU/mL penicillin and 100 IU/mL streptomycin at 37 °C under 5% CO₂. 3T3-L1 cells (2×10^3) or HepG2 cells (5×10^5) were plated onto 96-well plate (100 ml/well) and incubated for 24 h. After treated with compound (**3a** or **3f**) for 24 h, the cells were added 100 ml MTT (0.5 mg/mL) and incubated for 4 h. Then 100 ml DMSO was added to dissolve the blue insoluble MTT formazan. Finally, the absorbance was measured at 570 nm using a microplate reader. Each sample was performed in triplicate.

4.7. Statistical analysis

All data were presented as mean \pm SD. One-way ANOVA was performed to evaluate the difference between groups. $p < 0.05$ was considered significant.

Disclosure statement

No potential conflict of interest was reported by the author(s).

Funding

This work was financially supported by the National Natural Science Foundation of China [No. 81803390], Natural Science Foundation of Guangdong Province [No. 2021A1515010221], Special Fund Project of Science and Technology Innovation Strategy of Guangdong Province 2018 and 2020 [No. Jiangke (2018)352 and Jiangke (2020)182], Department of Education of

Guangdong Province [Nos. 2017KSYS010, 2019KZDXM035, 2021KCXTD044, 2021KTSCX135], Special Funds for the Cultivation of Guangdong College Students' Scientific and Technological Innovation ("Climbing Program" Special Funds, pdjh2021a0504) and Jiangmen City Science and Technology Basic Research Project [No. 2020030101030005457].

ORCID

Dong-Li Li  <http://orcid.org/0000-0001-9955-2304>

References

- Silva FSG, Oliveira PJ, Duarte MF. Oleanolic, ursolic, and betulinic acids as food supplements or pharmaceutical agents for type 2 diabetes: promise or illusion? *J Agric Food Chem* 2016;64:2991–3008.
- Saxena AR, Gorman DN, Esquejo RM, et al. Danuglipron (PF-06882961) in type 2 diabetes: a randomized, placebo-controlled, multiple ascending-dose phase 1 trial. *Nat Med* 2021;27:1079–87.
- Proença C, Ribeiro D, Freitas M, Fernandes E. Flavonoids as potential agents in the management of type 2 diabetes through the modulation of α -amylase and α -glucosidase activity: a review. *Crit Rev Food Sci Nutr* 2021;1–71. DOI:10.1080/10408398.2020.1862755
- Kokil GR, Veedu RN, Ramm GA, et al. Type 2 diabetes mellitus: limitations of conventional therapies and intervention with nucleic acid-based therapeutics. *Chem Rev* 2015;115:4719–43.
- Forouhi NG, Wareham NJ. Epidemiology of diabetes. *Medicine* 2014;42:698–702.
- Brás NF, Santos-Martins D, Fernandes PA, Ramos MJ. Mechanistic pathway on human α -glucosidase maltase-glucoamylase unveiled by QM/MM calculations. *J Phys Chem B* 2018;122:3889–99.
- Dhital S, Warren FJ, Butterworth PJ, et al. Mechanisms of starch digestion by α -amylase-structural basis for kinetic properties. *Crit Rev Food Sci Nutr* 2017;57:875–92.
- Shahzad D, Saeed A, Larik FA, et al. Novel C-2 symmetric molecules as α -glucosidase and α -amylase inhibitors: design, synthesis, kinetic evaluation, molecular docking and pharmacokinetics. *Molecules* 2019;24:1511.
- Elferink H, Bruekers JPJ, Veeneman GH, Boltje TJ. A comprehensive overview of substrate specificity of glycoside hydrolases and transporters in the small intestine: "a gut feeling". *Cell Mol Life Sci* 2020;77:4799–826.
- Liu J. Oleanolic acid and ursolic acid: Research perspectives. *J Ethnopharmacol* 2005;100:92–4.
- Sultana N, Ata A. Oleanolic acid and related derivatives as medicinally important compounds. *J Enzyme Inhib Med Chem* 2008;23:739–56.
- Pollier J, Goossens A. Oleanolic acid. *Phytochemistry* 2012;77:10–5.
- Castellano JM, Guinda A, Delgado T, et al. Biochemical basis of the antidiabetic activity of oleanolic acid and related pentacyclic triterpenes. *Diabetes* 2013;62:1791–9.
- Loza-Rodríguez H, Estrada-Soto S, Alarcón-Aguilar FJ, et al. Oleanolic acid induces a dual agonist action on PPAR γ / α and GLUT4 translocation: a pentacyclic triterpene for

- dyslipidemia and type 2 diabetes. *Eur J Pharmacol* 2020;883:173252.
15. Meng YQ, Nie HH, Wang XC, et al. Synthesis and anti-tumor activity of oleanolic acid derivatives. *Acta Pharm Sin* 2011;46:1215–20.
 16. Bednarczyk-Cwynar B, Zaprutko L, Marciniak J, et al. The analgesic and anti-inflammatory effect of new oleanolic acid acyloxymino derivative. *Eur J Pharm Sci* 2012;47:549–55.
 17. Ma CM, Nakamura N, Hattori M. Chemical modification of oleanene type triterpenes and their inhibitory activity against HIV-1 protease dimerization. *Chem Pharm Bull* 2000;48:1681–8.
 18. Chen J, Liu J, Zhang LY, et al. Pentacyclic triterpenes. Part 3: synthesis and biological evaluation of oleanolic acid derivatives as novel inhibitors of glycogen phosphorylase. *Bioorg Med Chem Lett* 2006;16:2915–9.
 19. Bednarczyk-Cwynar B, Zaprutko L. Recent advances in synthesis and biological activity of triterpenic acylated oximes. *Phytochem Rev* 2015;14:203–31.
 20. Zhong YY, Chen HS, Wu PP, et al. Synthesis and biological evaluation of novel oleanolic acid analogues as potential α -glucosidase inhibitors. *Eur J Med Chem* 2019;164:706–16.
 21. Wu PP, He H, Ma H, et al. Oleanolic acid indole derivatives as novel α -glucosidase inhibitors: synthesis, biological evaluation, and mechanistic analysis. *Bioorg Chem* 2021;107:104580.
 22. Chen X, Gao M, Jian R, et al. Design, synthesis and α -glucosidase inhibition study of novel embelin derivatives. *J Enzyme Inhib Med Chem* 2020;35:565–73.
 23. Chen P, Zhang Q, Dang H, et al. Screening for potential new probiotic based on probiotic properties and α -glucosidase inhibitory activity. *Food Control* 2014;35:65–72.
 24. Matsui T, Ueda T, Oki T, et al. Alpha-Glucosidase inhibitory action of natural acylated anthocyanins. 1. Survey of natural pigments with potent inhibitory activity. *J Agric Food Chem* 2001;49:1948–51.
 25. Han L, Fang C, Zhu R, et al. Inhibitory effect of phloretin on α -glucosidase: kinetics, interaction mechanism and molecular docking. *Int J Biol Macromol* 2017;95:520–7.
 26. Chi G, Wang L, Chen B, et al. Polyoxometalates: study of inhibitory kinetics and mechanism against α -glucosidase. *J Inorg Biochem* 2019;199:110784.
 27. Taha M, Imran S, Ismail NH, et al. Biology-oriented drug synthesis (BIODS) of 2-(2-methyl-5-nitro-1H-imidazol-1-yl)ethyl aryl ether derivatives, *in vitro* α -amylase inhibitory activity and *in silico* studies. *Bioorg Chem* 2017;74:1–9.
 28. Taha M, Javid MT, Imran S, et al. Synthesis and study of the α -amylase inhibitory potential of thiaziazole quinoline derivatives. *Bioorg Chem* 2017;74:179–86.
 29. Hameed S, Kanwal F, Seraj R, et al. Synthesis of benzotriazoles derivatives and their dual potential as α -amylase and α -glucosidase inhibitors *in vitro*: Structure-activity relationship, molecular docking, and kinetic studies. *Eur J Med Chem* 2019;183:111677.
 30. Wang GC, Wang J, Xie ZZ, et al. Discovery of 3,3-di(indolyl)indolin-2-one as a novel scaffold for α -glucosidase inhibitors: *in silico* studies and SAR predictions. *Bioorg Chem* 2017;72:228–33.
 31. Lin P, Zeng JC, Chen JG, et al. Z.P. Yin, Synthesis, *in vitro* inhibitory activity, kinetic study and molecular docking of novel N-alkyl-deoxynojirimycin derivatives as potential α -glucosidase inhibitors. *J Enzym Inhib Med Ch* 2020;35:1879–90.
 32. Floris S, Fais A, Medda R, et al. *Washingtonia filifera* seed extracts inhibit the islet amyloid polypeptide fibrils formations and α -amylase and α -glucosidase activity. *J Enzyme Inhib Med Chem* 2021;36:517–24.
 33. Wang GC, Peng ZY, Wang J, et al. Synthesis, *in vitro* evaluation and molecular docking studies of novel triazine-triazole derivatives as potential α -glucosidase inhibitors. *Eur J Med Chem* 2017;125:423–9.
 34. Ali F, Khan KM, Salar U, et al. Hydrazinyl arylthiazole based pyridine scaffolds: Synthesis, structural characterization, *in vitro* α -glucosidase inhibitory activity, and *in silico* studies. *Eur J Med Chem* 2017;138:255–72.
 35. Saleem F, Kanwal KM, Khan S, Chigurupati, et al. Synthesis of azachalcones, their α -amylase, α -glucosidase inhibitory activities, kinetics, and molecular docking studies. *Bioorg. Chem* 2020;106:104489.
 36. Liu D, He WG, Wang ZH, et al. Design, synthesis and biological evaluation of 3'-benzylated analogs of 3'-epi-neoponkoranol as potent α -glucosidase inhibitors. *Eur J Med Chem* 2016;110:224–36.
 37. Islam MS, Barakat A, Al-Majid AM, et al. A concise synthesis and evaluation of new malonamide derivatives as potential α -glucosidase inhibitors. *Bioorg Med Chem* 2016;24:1675–82.